



Integration of remote sensing techniques for monitoring desertification in Mexico

Rocio Becerril-Piña, Carlos Díaz-Delgado, Carlos Alberto Mastachi-Loza & Enrique González-Sosa

To cite this article: Rocio Becerril-Piña, Carlos Díaz-Delgado, Carlos Alberto Mastachi-Loza & Enrique González-Sosa (2016): Integration of remote sensing techniques for monitoring desertification in Mexico, Human and Ecological Risk Assessment: An International Journal

To link to this article: <http://dx.doi.org/10.1080/10807039.2016.1169914>



Accepted author version posted online: 04 Apr 2016.



Submit your article to this journal [↗](#)



View related articles [↗](#)



View Crossmark data [↗](#)

Integration of remote sensing techniques for monitoring desertification in Mexico

Rocio Becerril-Piña^{1*}, Carlos Díaz-Delgado¹, Carlos Alberto Mastachi-Loza¹ and Enrique González-Sosa²

¹ Centro Interamericano de Recursos del Agua (CIRA), Red Lerma (México), Facultad de Ingeniería, Universidad Autónoma del Estado de México. Cerro de Coatepec s/n, Ciudad Universitaria, Toluca 50130, México. Tel. and Fax: +52 722 296 55 50, e-mails: rbecerrilp@uaemex.mx, cdiazd@uaemex.mx, cmastachil@uaemex.mx

² Laboratorio de Hidráulica, Facultad de Ingeniería, Universidad Autónoma de Querétaro. Cerro de las Campanas, s/n, Santiago de Querétaro 76010, Tel. and Fax: +52 442 192 12 00, e-mail: egs@uaq.mx

* Address Correspondence to Rocio Becerril-Piña, e-mail: rbecerrilp@uaemex.mx

ACKNOWLEDGMENTS

This research was sponsored by the Mexican Environmental and Natural Resources Secretariat (SEMARNAT) and the National Council for Science and Technology (CONACyT) in the research project “Desertification indices of physical and/or biophysical basis” (108282) and project “Hydrometeorological model for identifying in real time areas susceptible to fire risk in order to support the protection of ecosystems and their biodiversity” The first author also wants to thank CONACyT for the scholarship (172784) in the Water Sciences postgraduate program at the Centro Interamericano de Recursos del Agua, Universidad Autónoma del Estado de México.

ABSTRACT

Desertification is considered one of the most serious threats to arid, semiarid, and sub-humid environments. In this study, several remote sensing techniques were integrated for monitoring desertification in a semiarid region of the central Mexican plateau (state of Querétaro). Landsat TM images were used to compute the Normalized Difference Vegetation Index (NDVI), Bare-Soil Index (BSI), and albedo (α). A change vector analysis (CVA) examined changes in the direction and magnitude of indicators during the 1993-2011 period in order to detect degradations or improvements in land conditions over a period of time. In addition, a desertification degree index (DDI) was applied based on the NDVI- α relationship. The results indicated that in the semiarid zone of the state of Querétaro, 48.3% of land use corresponds with agricultural areas; 2.7% of the area does not present any degree of desertification, while 49% presents the following degrees of desertification: 5.5% extreme, 10.9% severe, 18.9% moderate, and 13.7% low. The DDI applied in this approach for evaluating this phenomenon at the regional and municipal level is an effective tool for identifying areas at risk of desertification, in addition to monitoring changes in the degree or direction of desertification.

Key words:

desertification, Landsat, NDVI, albedo, CVA

Received: 14 Oct 2015

Accepted: 20 Mar 2016

1. INTRODUCTION

Desertification is considered one of the most serious threats to arid, semiarid, and sub-humid environments. These areas represent 40% of the world's land surface area, and currently, over 250 million people are at risk of being affected by this phenomenon (World Meteorological Organization. 2005). The United Nations Conference on Environment and Development (UNCED) defines desertification as land degradation in arid, semiarid, and dry sub-humid areas as a result of several factors, including climatic variations and human activities (Assembly 1994). The spatial heterogeneity and temporal dynamics of desertification lead to decreases in land productivity and biodiversity and as a consequence, potentially threaten the economic viability of a region (Mouat *et al.* 1997). The environmental and socio-economic impacts of desertification are reflected in the abandonment of productive lands and migration of populations (Schwartz and Notini 1994) towards more adequate areas for agriculture or raising livestock.

In Mexico, drylands make up approximately 65% of the land surface, including xeric, hyper-arid, arid, semiarid, and sub-humid environments (PHI-UNESCO and CAZALAC 2010), and are inhabited by 30% of the country's population (INEGI 2010). According to the data from Secretariat of Environment and Natural Resources of Mexico (SEMARNAT) (SEMARNAT-CP 2002), 45% of the country's soil area shows some kind of following degradation: chemical degradation (18%), water erosion (12%), wind erosion (9%), or physical degradation (6%). These are associated with agricultural and stockbreeding activities, the loss of vegetation cover, and urbanization. Thus, soil degradation references processes induced by human activities that provoke a decrease in biological productivity or diversity, affecting the current, and/or future capacity of a system to maintain human life (Olceman 1988); although this should not be

confused with land degradation, because it is only one of the many processes that contribute to the desertification of an area.

In this sense, the phenomenon of desertification is a dynamic process that is influenced by several biophysical and socio-economic factors (Reynolds and Smith 2002; Veron *et al.* 2006), such as deforestation and soil degradation, among others. In particular, water erosion and loss of vegetation cover are the most visible symptoms of losses in soil fertility (Pulido and Bocco 2011). However, in some regions, one of the greatest difficulties in confronting desertification is the identification of the process in its varying stages, as its manifestation is often not evident by plain sight (Abraham and Torres 2007). Numerous methods exist for determining the degree of desertification and its causes (Veron *et al.* 2006; Pulido and Bocco 2011). In this sense, there is an awareness of the need to use indicators and reference real data in order to achieve an adequate evaluation and monitoring of the components contributing towards desertification processes (Abraham 2009).

In this study, an indicator is defined as a parameter that provides information and describes the state of a determined phenomenon (OECD 2003), whereby a series of indicators allows for the synthesis of complex phenomena, in this case desertification, so that information may be shared among the affected population and decision makers.

In selecting desertification indicators, it is known that climatic variations and human activities lead to changes in land surface conditions that contribute towards this process and may be measured by examining reductions in vegetation cover, density, and biomass (Sivakumar 2007), in addition to assessing changes in vegetation pattern and structure resulting from increasing spatial and temporal heterogeneity of water or nutrients (Dunkerley 2000). Vegetation dynamics

can also induce a change in soil properties, both physical and chemical, thus affecting the micrometeorological conditions of the land surface (Xu *et al.* 2009; Pan and Li 2013). These changes in the state of the land surface create a notable spectral signature capable of being captured by remote sensors, therefore, allowing a quantitative evaluation of desertification at varying scales through indices derived from satellite images (Collado *et al.* 2002; Xu *et al.* 2009; Higginbottom and Symeonakis 2014; Becerril-Piña *et al.* 2015).

For example, multispectral satellite imagery, such as Landsat images, is a useful source of multi-temporal data for long-term analyses of surface processes (Liberti *et al.* 2009), enabling an exhaustive analysis of this phenomenon. In this case, change in vegetation is one of the most used indicators for analyzing desertification (Karnieli and Dall'Olmo 2003). Several specific indices for measuring these changes are the Normalized Difference Vegetation Index (NDVI), which monitors changes in the surface vegetation cover, and the Soil-Adjusted Vegetation Index (SAVI), which characterizes vegetation in semiarid zones through the use of a soil-adjustment factor that varies between 0 and 1 (Huete 1988).

Additionally, loss of soil fertility can be estimated with indicators that quantify the increase or decrease in soil surface area devoid of vegetation or the texture of the surface layer (Rikimaru *et al.* 2002; Xiao *et al.* 2006). Therefore, an index composed of indicators that would simultaneously take into account changes in vegetation cover, soil characteristics, or meteorological conditions through time and space could serve in the identification and assessment of desertification (Helldén 2008; Xu *et al.* 2009). This study utilizes the albedo and vegetation indices as part of an initial approach to the spatial-temporal evaluation of desertification processes. Moreover, it is particularly important to obtain a general panorama of

the affected areas in order to connect regional and local processes with the global dimensions of desertification (Hill *et al.* 2008).

For this reason, the analysis of desertification processes in Mexico at a regional and municipal level is of critical importance. In summary, the aim of this work was to integrate indicators derived from remote sensing data that allow the detection of areas at risk of desertification in order to evaluate regional processes and establish a baseline for this phenomenon, thereby facilitating subsequent comparisons and the design and implementation of prevention programs to combat desertification.

2. METHODOLOGY

There are numerous methods for evaluating desertification by remote sensing. Xie (2014) classified these into the following three categories: visual interpretation (Huang and Siegert 2006), classification algorithms (Hadeel *et al.* 2010), and spectral mixture analysis (Dawelbait and Morari 2012). In this study, two techniques based on classification by algorithm were integrated, the change vector analysis (CVA) and a regression model based on the vegetation index and albedo relationship, which allowed for desertification to be easily classified and monitored over time.

2.1. Study Area

In order to apply the proposed approach, a semiarid portion of the central Mexican plateau was selected, forming part of the state of Querétaro. The study area is located in the central northern region of the country and corresponds to the southern portion of the Chihuahuan desert between 21°05'–20°17' N and 99°25'–100°33' W (Figure 1), encompassing an area of 3,647 km² and including the municipalities of Querétaro, El Marqués, San Juan del Río,

Tequisquiapan, Ezequiel Montes, Corregidora, Tolimán, Colón, and Cadereyta. In 2010, the region had a population of 1,827,000 inhabitants (INEGI 2010). Overall, the regional climate corresponds to semiarid with an average annual temperature ranging from 12°C to 18°C, and annual rainfall varies between 450 and 620 mm with an average of 550 mm. The vegetation is mainly composed of shrubs averaging 4 m in height, and the main species are *Ipomea murucoides*, *Bursera* sp., *Lysiloma* sp., *Opuntia* sp., *Acacia* sp., and several cacti, including *Myrtillocactus geometrizans* (CONCYTEQ 2001). According to the map of land use and vegetation (INEGI 2011), 37.9% of the surface was composed of grass-shrub, 42.7% of agricultural zones, 15.3% of urban zones, 3.9% of forests, and only 0.2% of water bodies.

In this region of Querétaro, several nationally important socioeconomic and particularly demographic dynamics have occurred. During the 1980–2000 period Querétaro state presented the greatest growth in number of residents, doubling its population from 739,605 to 1,404,306 inhabitants (INEGI 2010). This growth may be considered a result of industrialization processes and the proximity of the region to Mexico City and has created migratory flows that have caused significant economic and social impacts to the region. Therefore, Querétaro is a zone of great agricultural, stockbreeding, and industrial significance at the national level and is simultaneously facing an accelerated and disordered urban growth, mainly in the suburban zone of Querétaro City (POEREQ 2009).

2.2. Data Acquisition

As this study consisted in the integration of indicators based on remote sensing data, the reflectivity values from Landsat images were extracted, which may be related to biophysical or

physical aspects of the desertification processes and were used for calculating later indices. Two Landsat Thematic Mapper 5 (TM) scenes were downloaded (<http://earthexplorer.usgs.gov/>) for April 18, 1993 and April 4, 2011 (path 27, row 46). These were selected of due to the high quality of the data (cloud free).

In this sense, with the goal of analyzing periods in which hydrological conditions would be comparable, the rainfall record for the study area was also considered. Similar levels of rainfall were reported for both selected periods (April 1993 and April 2011), thereby minimizing uncertainty in the comparison of results. In Figure 2, the daily rainfall records are shown for the study area. Records were analyzed from 1980 to 2011, and during this period an annual average rainfall of 571 mm was obtained for the region.

To determinate the dynamic land cover we used data series from the National Institute of Statistics and Geography (INEGI, for its initials in Spanish; Instituto Nacional de Estadística y Geografía), specifically Series II 1993 (INEGI 1993) and Series V 2011 (INEGI 2011). The following six categories of land use were established: water body, urban zone, forest, rainfed agriculture, irrigation agriculture, and grass-shrub cover.

2.3. Data Pre-processing

For multitemporal analyses using images data must be calibrated in order for the selected variables to be comparable to one another. The radiometric correction or conversion to reflectance is preferable for the majority of multitemporal applications and for a variety of purposes (Chander *et al.* 2009; Hansen and Loveland 2012). Therefore, for all images, a radiometric characterization and calibration were performed as a prerequisite for ensuring high-

quality data (Chander *et al.* 2009) in order to detect and quantify changes at the land surface. The conversion of digital numbers to reflectivity for each band (p_λ) was done by calculating the spectral radiance (L_λ) (Equation 1).

$$L_\lambda = (L_{max\lambda} - L_{min\lambda} / Q_{cal\ max} - Q_{cal\ min}) * DN + L_{min} \quad (1)$$

where L_{max} and L_{min} are constants for each band, DN the digital image numbers, and Q_{calmin} and Q_{calmax} the minimum and maximum quantized calibrated pixel values corresponding to L_{min} and L_{max} , respectively.

Equation 2 was used to convert the spectral radiance to reflectance, expressed in values ranging from 0 to 1, as follows:

$$\rho_\lambda = \pi * L_\lambda * d^2 / ESUN_\lambda * \cos\theta \quad (2)$$

where p_λ is the top of atmosphere reflectance (or TOA reflectance) (unitless), L_λ the spectral radiance, $ESUN_\lambda$ the mean exoatmospheric solar irradiance of each band ($Wm^{-2} \mu m$), θ the solar elevation angle (degrees), and d the Earth-Sun distance (Allen *et al.* 1998).

Finally, in order to reduce distortions caused by the atmosphere, an atmospheric correction was carried out with the ATMOSC module in Idrisi TerrSet (Clark Labs), using the Cos(t) model (Chavez 1996).

The satellite information and databases were processed in Idrisi TerrSet and ArcMap 9.3. Mosaics were constructed for bands 1, 2, 3, 4, 5, and 7, and were georeferenced to the WGS84 datum, UTM projection Zone 14 N, with a spatial resolution of 30 m.

2.4. Establishment of Indicators

For 1993 and 2011 the following indices were calculated to evaluate presence and direction of desertification: Bare Soil Index (BSI), Normalized Difference Vegetation Index (NDVI), Soil Adjusted Vegetation Index (SAVI), and albedo (α). In the first phase, the dynamic of changes in land cover throughout the study area was evaluated by a change vector analysis (CVA) (Lorena *et al.* 2002; Kuzera *et al.* 2005), which assesses the direction and magnitude of change. In the second phase, relevant indicators were integrated in a reflectance analysis (Pan and Li 2013) (Figure 3) in order to estimate the degree of desertification based on the NDVI- α relationship.

The BSI is commonly used to evaluate increases in desertification processes along a gradient of bare soil exposure (Rikimaru *et al.* 2002; Xiao *et al.* 2006), and it is described by the following relationship (Equation 3):

$$BSI = ((\rho_{SWIR} + \rho_R) - (\rho_{NIR} + \rho_B)) / ((\rho_{SWIR} + \rho_R) + (\rho_{NIR} + \rho_B)) * 100 + 100 \quad (3)$$

where ρ is the reflectance, *SWIR* the shortwave infrared band, *R* the red band, *NIR* the near infrared band, and *B* the blue band.

The NDVI (Equation 4) and SAVI (Equation 5) vegetation indices, commonly used to indirectly describe the condition of vegetation cover, were calculated in order to identify vegetative changes on the land surface and select the most appropriate index given the heterogeneity and characteristics inherent to this region.

$$NDVI = (\rho_{NIR} - \rho_R) / (\rho_{NIR} + \rho_R) \quad (4)$$

$$SAVI = ((\rho_{NIR} - \rho_R) / (\rho_{NIR} + \rho_R + L)) * (1 + L) \quad (5)$$

where ρ is the reflectance, *NIR* the near infrared band, *R* the red band, and *L* the soil-adjustment factor at a value 0.5, as proposed by Huete (1988).

2.4.1. Analysis of land use changes

It was important to obtain a general panorama of the affected areas, which is relevant for the evaluation and monitoring of desertification in a global context in addition to understanding its relevance for other locally occurring environmental processes (Hill *et al.* 2008). Several studies that have assessed landscape dynamics in areas affected by desertification consider changes in land use to be an important factor influencing further land degradation (Foley *et al.* 2005; Hill *et al.* 2008). To achieve this and in order to evaluate the direction and magnitude of the land surface changes that have occurred in the study area between 1993 and 2011, a CVA was applied using a vegetation index and the BSI.

CVA is a multivariate technique for analyzing spectral bands or derived indices pixel by pixel by plotting these on two axes of a Cartesian plane, thereby assessing changes that have occurred between a reference (T_1) and target date (T_2) (Lorena *et al.* 2002; Dawelbait and Morari 2012). The direction of change represents the type of change (θ) that occurred in a pixel from T_1 to T_2 , where each vector is a function of the combination of the either positive or negative changes (Equation 6). Generally, the number of categories of the change is equal to 2^n , where n is the number of spectral bands or derived indices. Vectors with resulting angles of between 90° and 180° represent an increase in vegetation cover (regrowth); angles of 270° to 360° relate to the brightness of the pixels and correspond with bare soil (degradation). Finally, angles of 0° to 90° and 180° to 270° represent persistence, or pixels without evidence of increase or decrease in vegetation or bare soil (Lorena *et al.* 2002). Angles were calculated from the following equation:

$$\tan \theta = (Baresoil_1 - Baresoil_2) / (Vegetation_1 - Vegetation_2) \quad (6)$$

Finally, the magnitude (M) represents the intensity of change and is deduced from the Euclidian distance of a vector, calculated from the reference points of the two selected dates

(Equation 7). Its intensity may be classified into four categories: low, medium, high, or extreme (Figure 3). M was calculated from the following equation:

$$M = \sqrt{(Vegetation_1 - Vegetation_2)^2 + (Baresoil_1 - Baresoil_2)^2} \quad (7)$$

2.4.2. Change detection accuracy assessment

The accuracy of the map generated by the CVA technique was also evaluated. A random sampling of 303,397 pixels was performed. The corresponding values for NDVI and BSI were extracted, and each pixel was classified as “change” or “no change.” Finally, a confusion matrix was constructed, and the levels of agreement were calculated according to the Kappa coefficients (Cohen 1960).

The confusion matrix was constructed, and the levels of agreement were calculated according to the Kappa coefficients (Cohen 1960). Values lower than 0.4 present poor agreement between images, 0.4 to 0.55 fair agreement, 0.55 to 0.7 good agreement, 0.7 to 0.85 very good agreement, and finally, values higher than 0.85 indicate excellent agreement (Monserud and Leemans 1992)

2.4.3. Reflectance analysis and desertification degree index (DDI)

Several authors have related the degradation of vegetation cover and its effect on the albedo (α) and climate (Charney *et al.* 1977; Robinove *et al.* 1981; Liang 2001; Xu *et al.* 2009). Charney *et al.* (1977) mentions that for semiarid areas, an increase in α is related to changes in vegetation that resulted in lower precipitation. Also, Robinove *et al.* (1981) suggest that in semiarid zones when the α decreases an improvement in the soil quality can be recognized. Meanwhile, an increases in α indicates degradation, considering that α is not only a function of vegetation cover but also of soil moisture. In this context, the formulation of an indicator that

would integrate the spatial-temporal reflectivity of the vegetation and the α of the surface area was proposed in order to determine the rate of desertification.

To calculate the α , a model proposed by Liang (2001) was used (Equation 8):

$$\alpha = 0.356 * \rho_1 + 0.130 * \rho_3 + 0.373 * \rho_4 + 0.085 * \rho_5 + 0.072 * \rho_7 - 0.0018 \quad (8)$$

where $\rho_1, \rho_3, \rho_4, \rho_5$, and ρ_7 represent the reflectance of the band 1, 3, 4, 5, and 7 of Landsat TM image, respectively.

The NDVI and α values were normalized considering the maximum ($_{max}$) and minimum ($_{min}$) value of each as a reference (Equation 9 and Equation 10):

$$NDVI_N = ((NDVI - NDVI_{min}) / (NDVI_{max} - NDVI_{min})) * 100 \quad (9)$$

$$Albedo_N = ((Albedo - Albedo_{min}) / (Albedo_{max} - Albedo_{min})) * 100 \quad (10)$$

A regressive model was built based on the NDVI- α relationship (Pan and Li 2013), for the year 2011, and pixel values for three conditions were extracted: bare soil, partially covered soil, and vegetation cover. The Jenks natural breaks method (ArcMap 9.3) was used to classify data values into five degrees of desertification: null, low, moderate, severe, and extreme. Several authors have successfully used this method to classify natural phenomena (Becerril-Piña *et al.* 2015; Han *et al.* 2015; Yaduvanshi *et al.* 2015). This method identifies the break points between categories with the Jenks' optimization algorithm, which is based on the nature of the data and its inherent groupings. The points where difference is maximized are identified and used as the thresholds for each category (Jenks 1963).

3. RESULTS AND DISCUSSION

3.1. Land Use Dynamics

Figure 4 shows the changes in land cover over a period of 18 years in the semiarid region of Querétaro, using data from Series II (1993) and Series V (2011). In 1993, 70.6% of the surface was made up of grass-shrub (VI; 2567.9 km²), 19.5% agricultural zones (IV and V; 713.3 km²), 5.8% urban zones (II; 213.2 km²), 4% forests (III; 147.4 km²), and only 0.1% of water bodies (I; 5 km²). In contrast, by 2011, the urban areas have tripled in size, covering 15.3% (556.3 km²) of the state. These results are consistent with the economic and population growth of the region, as it is geographically located between the flow of commerce from Mexico City to northern Mexico and the United States. Land use changes in the region have evidenced the lack of a focused and orderly development and have resulted in the creation of dispersed urban areas that have triggered desertification and other social problems (Rello *et al.* 2002).

Grass-shrub vegetation lost almost half of its area (1,186 km²), and water bodies (for storage) increased by 4 %. Currently, agricultural zones represent 42.2 % (1,560 km²) of land area, where more than half of the cultivated land is sustained by rainfed agriculture. With respect to net gains and losses in land cover, grass-shrub was the only vegetation type that had a negative net change, as more than 70% of the existing area in 1993 was reclassified as agricultural and 23% as urban in 2011.

Given the spatial heterogeneity of this study area, a correlation analysis was performed with the aim of identifying the index that best represents the vegetation cover, volume, and vitality. Figure 5 shows the BSI-SAVI and BSI-NDVI correlations. The BSI-NDVI relationship presented a moderate negative correlation coefficient of $r=-0.75$ ($r^2=0.57$), and the BSI-SAVI had a correlation of $r=-0.70$ ($r^2=0.49$). There are several advantages and limitations to the use of vegetation indices for semiarid zones (Eisfelder *et al.* 2012), where the use of NDVI is

recommended for regions with an average index value of greater than 0.1 (Higginbottom and Symeonakis 2014). For this reason and based on the results, since an average value of 0.26 was found, it was decided that for this study the BSI-NDVI relationship would be used to analyze changes in land cover with respect to both magnitude and direction of change.

The CVA technique showed that changes mainly occurred at the limits of the urban areas and in grass-shrub, which indicate that these transition areas are highly sensitive to anthropogenic impacts, mainly due to land use changes. Of the study area, 76.2% remained the same or did not present an increase or decrease in vegetation cover or bare soil areas (persistence). Bare soil diminished and the vegetation cover increased in 16.1% (regrowth) of the area, while vegetation cover decreased and bare soil increased in 7.8% (degradation; Figure 6a) of the land area. In the areas with degradation, 46.7% showed low magnitude, 34.4% medium, and 18.8% high, and these were principally located along the industrial corridors of the cities of Querétaro and San Juan del Río. Areas presenting regrowth may be explained by the possible increase in land area with irrigation infrastructure (CONCYTEQ 2001). However, a greening of forests and grass-shrub can also be observed; this phenomenon may be the result of a high rainfall level (700 mm) in 2010.

The evaluation of the accuracy of the map generated by the CVA technique (Figure 6c) indicated that a good classification was performed for pixels with either “change” or “no change” (Monserud and Leemans 1992), as the resulting Kappa statistic had a value of 0.65. The producer’s accuracy for the “no change” class was 0.97, and the user’s accuracy for the “change” class was 0.63. Although the majority of pixels of the “change” class were appropriately classified, 27% of its pixels were incorrectly classified as “no change.” In contrast, the majority

of the pixels classified as “no change” were correctly classified, with only 3% being incorrectly classified.

This analysis allows for visualizing the changes over a period of time; however, care must be taken in its interpretation, and it is advisable to evaluate the water availability of an area through a historical rainfall analysis (Figure 2), since vegetation behavior may radically differ from dry to wet years, especially in semiarid areas (Karnieli *et al.* 2010)

3.2 Desertification Degree Index (DDI)

The desertification degree index (DDI) was derived from a reflectivity analysis, and the NDVI- α relationship showed a negative correlation with different types of desertification. Indeed, high albedo values corresponded to zones of low vegetation cover or bare soil. In fact, the regression model (Equation 11) presented a strong correlation $r=-0.92$ ($r^2=0.85$) between these characteristics. Three general conditions were identified: vegetation cover, partially covered, and bare soil. From these conditions, 401 random pixels were extracted to analyze the relationship NDVI- α (Figure 7a).

$$Albedo = -1.305 * NDVI + 65.93 \quad (11)$$

Pan and Li (2013) propose that the DDI (Equation 12) may be obtained from the NDVI- α relationship, as follows:

$$DDI = \varphi * NDVI - Albedo \quad (12)$$

where φ is the slope of the orthogonal lines found in the NDVI- α relationship or in this case, 0.766 (1/1.305 Equation 11). The natural breaks method allowed for the identification of the intervals, resulting in the following desertification categories: null for pixels with values of 35 to

66, low for 23 to 34, moderate for 14 to 22, severe for 5 to 13, and extreme for -64 to 4. The dispersion of the different desertification degrees was plotted, where it is observed that the pixels with a null or low degree of desertification also presented values of $NDVI > 70$ (normalized values). Meanwhile, some pixels with albedo values > 40 (normalized values) corresponded to an extreme degree of desertification (Figure 7b) and were composed of areas with low vegetation cover or bare soil.

3.3 Evaluating Desertification

After applying the DDI (equation 12), in order to avoid overestimating the degree of desertification, a mask was used to remove agricultural areas and water bodies (48.3% of the study area). The DDI revealed that 49% of the zone had undergone some degree of desertification, where 5.5% is classified as extreme and 10.7% as severe, mainly in urban areas and at their limits. Meanwhile, of the remaining area 18.9% is classified as moderate and 13.7% as low, mainly in grass-shrub and forested areas (Figure 8). Only 2.7% of the area does not present any degree of desertification, corresponding to the forested zones of the Cadereyta, Tolimán, Colón, and El Marqués municipalities. However, the results of the CVA indicated that there is a moderate degree of degradation bordering these regions and their transitional areas, which may be considered complementary and of importance to the evaluation of the desertification processes in these areas.

Table 1 shows a summary of the integrated indicators for remotely monitoring desertification processes. The analysis was regionally focused according to municipal divisions in order to be relevant for planning decisions at this level, considering that in Mexico, the municipality is the

basis of territorial division and of the political and administrative organization of the states. Furthermore, our approach responds to the fact that actions will require an integrated and participative approach from local stakeholders (Pulido and Bocco 2011). Rubio and Recatalá (2006) mention that at a local scale, physiography, soil types, land uses, cultural traditions, and land management are important factors that additionally influence the desertification process. Therefore, combating desertification is dependent upon understanding a wide range of spatial, temporal, cultural, socioeconomic, and environmental conditions specific to each region (Warren 2002). The presentation of these results at the municipal level is key in order for decision makers to be able to link these results with their efforts and other local projects or actions.

Although land and soil degradation are not synonymous, the aforementioned does play an important role in desertification, and the results of the SEMARNAT-CP (2003) soil degradation study were reviewed for Mexico for purposes of comparison. In general, it can be observed that forested areas of the Colón and Cadereyta municipalities had significant water erosion at high altitudes (Figure 1), in addition to extensive grazing and agricultural activities. Although the rate of change was low, the degree of desertification indicated vulnerability for this region. However, the main problem is observed in grass-shrub zones, where urbanization is the principal cause of land degradation (Marzluff and Ewing 2001) and is a product of regional industrial development. In addition to this, the city of Querétaro has undergone a physical degradation of its soil due to loss of productivity and topsoil from water erosion. Also, in most parts of the San Juan del Río municipality, soils exhibit signs of chemical degradation and decreasing organic matter content and fertility (SEMARNAT-CP 2002).

Finally, the DDI indicated that the municipalities with the greatest risk are Corregidora, Querétaro, and Ezequiel Montes, as more than 20% of their area is experiencing severe desertification. Therefore, these municipalities require a priority analysis and continued monitoring. Several areas currently present extreme rates of desertification caused by the removal of vegetation cover and land use changes, and these municipalities have also experienced an uncontrolled urban growth and an intensive industrial development.

Although visual interpretation is the main method of monitoring desertification patterns over time, the degrees of desertification were also confirmed through points of verification with the aid of Google Earth. Table 2 shows changes over the analyzed time period, occurring between 2000 and 2011. Even though the analysis period does not correspond with the Landsat TM data, it is important to point out that the results obtained in this analysis are compatible with the goal of confirming the land surface changes that have occurred in the area.

Finally, although the main objective of this study did not involve determining the driving forces of desertification, the rainfall analysis (Figure 2) does not show any change in average annual levels of rainfall (1993-2011 period). This suggests that the causes of desertification are anthropogenic in nature, and in this case, due to changes in land use resulting from the development of industrial and agricultural activities in the state. However, in this initial approach, sufficient elements were not included in the analysis in order to arrive at a conclusion regarding the driving forces of desertification. Thus, it is evident that future studies are both required and urgent in order to determine the causes and effects of desertification in the semiarid region of central Mexico, which could include both anthropogenic and climatological indicators.

4. CONCLUSIONS

In order to monitor the process of desertification over time, relevant indicators were integrated to facilitate its detection and monitoring by an easy, fast, and low cost method, that at the same time maximizes accuracy at a regional scale, pixel by pixel.

In this study, techniques based on classification methods derived from the use of multi-spectral and temporal satellite images, in addition to a regression model based on the NDVI- α relationship, allowed for the desertification of the central, semiarid region of Mexico to be classified.

Thus, the index (DDI) offered a panorama of the spatio-temporal changes in the study region in terms of vegetation cover, soil, climate, and water availability, by means of calculating the albedo. The CVA technique was also used to identify the direction and magnitude of change and may be integrated into desertification monitoring. The NDVI-BSI relationship facilitated the characterization of desertification and helped to identify zones of degradation or regrowth over time by qualitatively classifying the state of desertification and its direction and rate of change as low, medium, or high, as based on a pixel-by-pixel analysis of images for the study region. The analysis based on the NDVI- α relationship classified resulting values in five categories of desertification: null, low, moderate, severe, and extreme.

As straightforward as this approach is, it is still necessary to work with high-quality data and have knowledge of the area of interest and of the methodology and process in order to correctly interpret the results (Hein *et al.* 2011). For this reason, these kind of studies should be considered complimentary to local decision making, where actions plans may be designed and applied to take into account regional conditions and processes specific to the areas of study.

In particular, the results of the present case study of Querétaro give evidence of an extreme tendency towards desertification at urban centers and their outlying suburban areas. In identifying the areas most at risk, the cities of Querétaro and San Juan del Río were found to be the most vulnerable and affected. Thus, the indicators used in this approach to evaluate desertification at a regional scale can be considered to be effective tools for monitoring desertification and detecting emerging vulnerable zones, and this is a crucial first step in the design and implementation of action plans to combat desertification.

Finally, given both the temporal and spatial nature of this phenomenon, remote sensing is a useful, low cost tool for analysis at the municipal level, considering that in Mexico, specifically, the municipality is the basic unit of territorial division and of the political and administrative organization of the states. However, as previously mentioned, climate and socioeconomic indicators may be complementary to those used in this study and would allow for a more in-depth analysis.

6. REFERENCES

- Abraham E. 2009. Enfoque y evaluación integrada de los problemas de desertificación. *Zonas Áridas*. 13:9–24.
- Abraham EM and Torres LM. 2007. Estado del arte en el uso de indicadores y puntos de referencia en la lucha contra la desertificación y la sequía en América Latina y el Caribe. *Interciencia*. 32:827–833.
- Allen RG, Pereira LS, Raes D, *et al.* 1998. Crop evapotranspiration-Guidelines for computing crop water requirements-FAO Irrigation and drainage paper 56. FAO Rome. 300:6541.
- Assembly UG. 1994. Elaboration of an International Convention to Combat Desertification in countries experiencing serious drought and/or desertification, particularly in Africa. *AC*. 241:27.
- Becerril-Piña R, Mastachi-Loza CA, González-Sosa E, *et al.* 2015. Assessing desertification risk in the semi-arid highlands of central Mexico. *J Arid Environ*. 120:4–13.
- Chander G, Markham BL and Helder DL. 2009. Summary of current radiometric calibration coefficients for Landsat MSS, TM, ETM+, and EO-1 ALI sensors. *Remote Sens Environ*. 113:893–903.
- Charney J, Quirk WJ, Chow S-H, *et al.* 1977. A comparative study of the effects of albedo change on drought in semi-arid regions. *J Atmospheric Sci*. 34:1366–1385.

- Chavez PS. 1996. Image-based atmospheric corrections-revisited and improved. *Photogramm Eng Remote Sens.* 62:1025–1035.
- Cohen J, 1960. A coefficient of agreement for nominal scale. *Educ Psychol Meas.* 20:37-46.
- Collado AD, Chuvieco E and Camarasa A. 2002. Satellite remote sensing analysis to monitor desertification processes in the crop-rangeland boundary of Argentina. *J Arid Environ.* 52:121–133.
- CONCYTEQ. 2001. Uso del suelo y vegetación de la zona sur del estado de Querétaro.
- Dawelbait M and Morari F. 2012. Monitoring desertification in a Savannah region in Sudan using Landsat images and spectral mixture analysis. *J Arid Environ.* 80:45–55.
- Dunkerley D. 2000. Hydrologic effects of dryland shrubs: defining the spatial extent of modified soil water uptake rates at an Australian desert site. *J Arid Environ.* 45:159–172.
- Eisfelder C, Kuenzer C and Dech S. 2012. Derivation of biomass information for semi-arid areas using remote-sensing data. *Int J Remote Sens.* 33:2937–2984.
- Foley JA, DeFries R, Asner GP, *et al.* 2005. Global consequences of land use. *science.* 309:570–574.
- Hadeel A, Jabbar MT and Chen X. 2010. Application of remote sensing and GIS in the study of environmental sensitivity to desertification: a case study in Basrah Province, southern part of Iraq. *Appl Geomat.* 2:101–112.
- Han L, Zhang Z, Zhang Q, *et al.* 2015. Desertification assessments in the Hexi corridor of northern China's Gansu Province by remote sensing. *Nat Hazards.* 75:2715–2731.

- Hansen MC and Loveland TR. 2012. A review of large area monitoring of land cover change using Landsat data. *Remote Sens Environ.* 122:66–74.
- Hein L, De Ridder N, Hiernaux P, *et al.* 2011. Desertification in the Sahel: Towards better accounting for ecosystem dynamics in the interpretation of remote sensing images. *J Arid Environ.* 75:1164–1172.
- Helldén U. 2008. A coupled human–environment model for desertification simulation and impact studies. *Glob Planet Change.* 64:158–168.
- Higginbottom TP and Symeonakis E. 2014. Assessing Land Degradation and Desertification Using Vegetation Index Data: Current Frameworks and Future Directions. *Remote Sens.* 6:9552–9575.
- Hill J, Stellmes M, Udelhoven T, *et al.* 2008. Mediterranean desertification and land degradation: mapping related land use change syndromes based on satellite observations. *Glob Planet Change.* 64:146–157.
- Huang S and Siegert F. 2006. Land cover classification optimized to detect areas at risk of desertification in North China based on SPOT VEGETATION imagery. *J Arid Environ.* 67:308–327.
- Huete AR. 1988. A soil-adjusted vegetation index (SAVI). *Remote Sens Environ.* 25:295–309.
- INEGI. 1993. Conjunto de Datos Vectoriales de la Carta de Uso de Suelo y Vegetación, escala 1: 250,000, serie III continuo nacional [Internet]. Available from: <http://www.inegi.org.mx/geo/contenidos/reclnat/usosuelo/Default.aspx>

INEGI. 2010. II Censo de población y vivienda 2010. Indicadores Censo Gen Poblac Vivienda
Ed INEGI México.

INEGI. 2011. Conjunto de Datos Vectoriales de la Carta de Uso de Suelo y Vegetación, escala 1:
250,000, serie V continuo nacional [Internet]. Available from:
<http://www.inegi.org.mx/geo/contenidos/reclnat/usosuelo/Default.aspx>

Jenks GF. 1963. Generalization in statistical mapping. *Ann Assoc Am Geogr.* 53:15–26.

Karnieli A, Agam N, Pinker RT, *et al.* 2010. Use of NDVI and land surface temperature for
drought assessment: merits and limitations. *J Clim.* 23:618–633.

Karnieli A and Dall’Olmo G. 2003. Remote-sensing monitoring of desertification, phenology,
and droughts. *Manag Environ Qual Int J.* 14:22–38.

Kuzera K, Rogan J and Eastman JR. 2005. Monitoring vegetation regeneration and deforestation
using change vector analysis: Mt. St. Helens study area. In: ASPRS Annu Conf Baltim MD
[Internet].; [cited 2014 Nov 12]. Available from:
http://www.geog.ucsb.edu/~kuzera/kuzera_rogan_eastman_1.pdf

Liang S. 2001. Narrowband to broadband conversions of land surface albedo I: Algorithms.
Remote Sens Environ. 76:213–238.

Liberti M, Simoniello T, Carone MT, *et al.* 2009. Mapping badland areas using LANDSAT
TM/ETM satellite imagery and morphological data. *Geomorphology.* 106:333–343.

- Lorena RB, Santos JR, Shimabukuro YE, *et al.* 2002. A change vector analysis technique to monitor land use/land cover in sw Brazilian amazon: Acre state. PECORA 15-Integrating Remote Sens Glob Reg Local Scale.:8–15.
- Malila WA. 1980. Change vector analysis: an approach for detecting forest changes with Landsat. In: LARS Symp [Internet]. [cited 2014 Nov 12]; p. 385. Available from: http://docs.lib.purdue.edu/cgi/viewcontent.cgi?article=1386&context=lars_symp
- Marzluff JM and Ewing K. 2001. Restoration of fragmented landscapes for the conservation of birds: a general framework and specific recommendations for urbanizing landscapes. *Restor Ecol.* 9:280–292.
- Monserud RA and Leemans R. 1992. Comparing global vegetation maps with the Kappa statistic. *Ecological modelling*, 62:275-293.
- Mouat D, Lancaster J, Wade T, *et al.* 1997. Desertification evaluated using an integrated environmental assessment model. *Environ Monit Assess.* 48:139–156.
- OECD. 2003. OECD Environmental Indicators: Development, Measurement and Use. [Httpwwwoecdorgenvironmentindicators-Model-Outlooks24993546pdf](http://www.oecd.org/environment/indicators-Model-Outlooks24993546pdf) [Internet]. Available from: <http://www.oecd.org/environment/indicators-modelling-outlooks/24993546.pdf>
- Olcleman L. 1988. Guidelines for general assessment of the status of human-induced soil degradation. *Int Soil Ref Inf Cent ISRIC.*:88.
- Pan J and Li T. 2013. Extracting desertification from Landsat TM imagery based on spectral mixture analysis and Albedo-Vegetation feature space. *Nat Hazards.* 68:915–927.

- PHI-UNESCO, CAZALAC. 2010. Proyecto elaboración del mapa de zonas áridas, semiáridas y subhúmedas de América Latina y el Caribe.
- POEREQ. 2009. Programa de Ordenamiento Ecológico Regional del Estado de Querétaro. Periódico del Gobierno del Estado de Querétaro. CXLII.
- Pulido J and Bocco G. 2011. ¿Cómo se evalúa la degradación de tierras? Panorama global y local. *Interciencia*. 36:96–103.
- Rello F, Morales M, Davis B, *et al.* 2002. The rural non-farm economy and farm/non-farm linkages in Queretaro, Mexico. *Promot FarmNon-Farm Link Rural Dev Case Stud Afr Lat Am.*:61–95.
- Reynolds JF and Smith DS. 2002. Global desertification: do humans cause deserts. In *Dahlem Workshop Report Vol. 88*.
- Rikimaru A, Roy PS and Miyatake S. 2002. Tropical forest cover density mapping. *Trop Ecol.* 43:39–47.
- Robinove CJ, Chavez Jr PS, Gehring D, *et al.* 1981. Arid land monitoring using Landsat albedo difference images. *Remote Sens Environ.* 11:133–156.
- Rubio JL and Recatalá L. 2006. The relevance and consequences of Mediterranean desertification including security aspects. In: *Desertification Mediterr Reg Secur Issue*. Springer; p. 133–165.
- Schwartz ML and Notini J. 1994. *Desertification and migration: Mexico and the United States*. US Commission on Immigration Reform San Francisco, CA.

SEMARNAT-CP. 2002. Evaluación de la degradación del suelo causada por el hombre en la República Mexicana. Mem Nac Secr Medio Ambiente Recur Nat.

Sivakumar M. 2007. Interactions between climate and desertification. *Agric For Meteorol.* 142:143–155.

Veron S, Paruelo J and Oesterheld M. 2006. Assessing desertification. *J Arid Environ.* 66:751–763.

Warren A. 2002. Land degradation is contextual. *Land Degrad Dev.* 13:449–459.

World Meteorological Organization. 2005. Climate and land degradation. Geneva, Switzerland: WMO.

Xiao J, Shen Y, Tateishi R, *et al.* 2006. Development of topsoil grain size index for monitoring desertification in arid land using remote sensing. *Int J Remote Sens.* 27:2411–2422.

Xie ZH. 2014. Research Advance in Remote Sensing to Land Desertification Monitoring. In: Vol. 864. *Trans Tech Publ*; p. 2817–2820.











Xu D, Kang X, Qiu D, *et al.* 2009. Quantitative Assessment of Desertification Using Landsat Data on a Regional Scale – A Case Study in the Ordos Plateau, China. *Sensors.* 9:1738–1753.

Yaduvanshi A, Srivastava PK and Pandey A. 2015. Integrating TRMM and MODIS satellite with socio-economic vulnerability for monitoring drought risk over a tropical region of India. *Phys Chem Earth Parts ABC.*

Table 1. Summary of the land cover and integrated indicators to evaluate the desertification process at a municipal level in the semiarid zone of the state of Querétaro.

Municipalities		Corregidora 113.3 km ²	Querétaro 443 km ²	El Marqués 673 km ²	Colón 751 km ²	Tequisquiapan 200 km ²	San Juan del Río 336 km ²	Cadereyta 759.53 km ²	Ezequiel Montes 89 km ²	Tolimán 195.53 km ²
		Surface (%)								
Land uses (2011)	Water bodies	0.1	0.2	0.1	0.1	0.0	0.5	0.1	0.0	0.0
	Urban zone	29.7	35.9	8.2	2.0	6.0	14.5	9.7	5.8	4.3
	Forest	0.2	0.1	2.6	3.2	0.4	0.6	5.5	0.3	20.5
	Rainfed agriculture	22.3	26.1	32.0	25.9	39.1	36.2	23.2	26.2	6.7
	Irrigation agriculture	24.1	11.1	14.9	6.6	9.8	20.1	12.9	8.4	11.9
	Grass-shrub	23.7	26.6	42.2	62.2	44.7	28.0	48.4	59.4	56.6
Change Vector Analysis (1993-2011)	Persistence	53.9	63.5	73.3	86.5	81.6	69.1	81.3	84.1	78.9
	Low regrowth	14.5	18.1	12.1	8.3	12.3	15.3	15.9	12.8	19.8
	Medium regrowth	3.1	1.3	1.9	1.0	1.3	3.1	1.5	0.4	0.6
	High regrowth	0.6	0.5	0.6	0.4	0.6	1.6	0.1	0.1	0.0
	Low degradation	15.3	12.0	3.9	0.9	1.6	3.9	0.9	1.7	0.4
	Medium degradation	9.0	3.2	5.2	1.9	2.0	3.8	0.2	0.7	0.2
Desertification (α - NDVI)	High degradation	3.5	1.4	3.1	1.0	0.5	3.2	0.0	0.2	0.0
	Null	0.0	0.1	1.8	2.6	0.2	0.3	4.3	0.3	11.8
	Low	7.6	7.6	13.2	17.7	11.7	7.1	13.5	15.4	33.1
	Moderate	12.1	14.4	14.7	26.2	17.5	11.0	23.1	18.9	23.4
	Severe	13.6	17.0	8.0	9.9	8.2	9.7	12.7	8.9	7.0
Extreme	11.5	17.2	4.5	1.6	2.4	5.3	4.8	4.0	1.5	

Table 2. Verification points for the integration of the CVA analysis and DDI in the semiarid region of the state of Querétaro.

Image (200 m X 200 m)		Categories NDVI- α	Description
Before (2000)	After (2011)		
		Null	These areas correspond to high altitude, forested zones. According to the CVA, some areas present medium and high regrowth.
(20° 55.60' N 100° 7.84' W)			
		Low	This category was identified for patches of vegetation or islands of grass-shrub. According to the CVA, these areas represent zones of low regrowth, which are a result of regional reforestation programs. There are also several zones with medium degradation due to pressure from local inhabitants, who harvest wood for domestic use.
(20° 47.38' N 100° 9.58' W)			
		Moderate	These areas mainly correspond to areas that have been converted from agriculture to grass-shrub. Some abandoned terrains have low regrowth, considering that the regeneration of this type of vegetation is slow. However, areas with low and medium degradation were also identified due to changes in land use from grass-shrub to agriculture, or due to harvesting of wood.
(20° 41.81' N 100° 12.02' W)			
		Severe	In these areas, drastic changes have occurred from grass-shrub to agriculture, and also represent zones that were located close to cities and dramatically changed to urban land uses. Due to this, the CVA classifies these as severely degraded.
(20° 38.87' N 100° 8.55' W)			
		Extreme	In this category, urban areas and highways are found, in addition to a quarry that is highly exploited by the Cadereyta municipality. The results of CVA indicate that these zones are extremely degraded, which is corroborated by the evident extension and growth of urban areas that have begun to replace the remaining relicts of vegetation.
(20° 55.6' N 100° 7.84' W)			

FIGURES AND TABLES

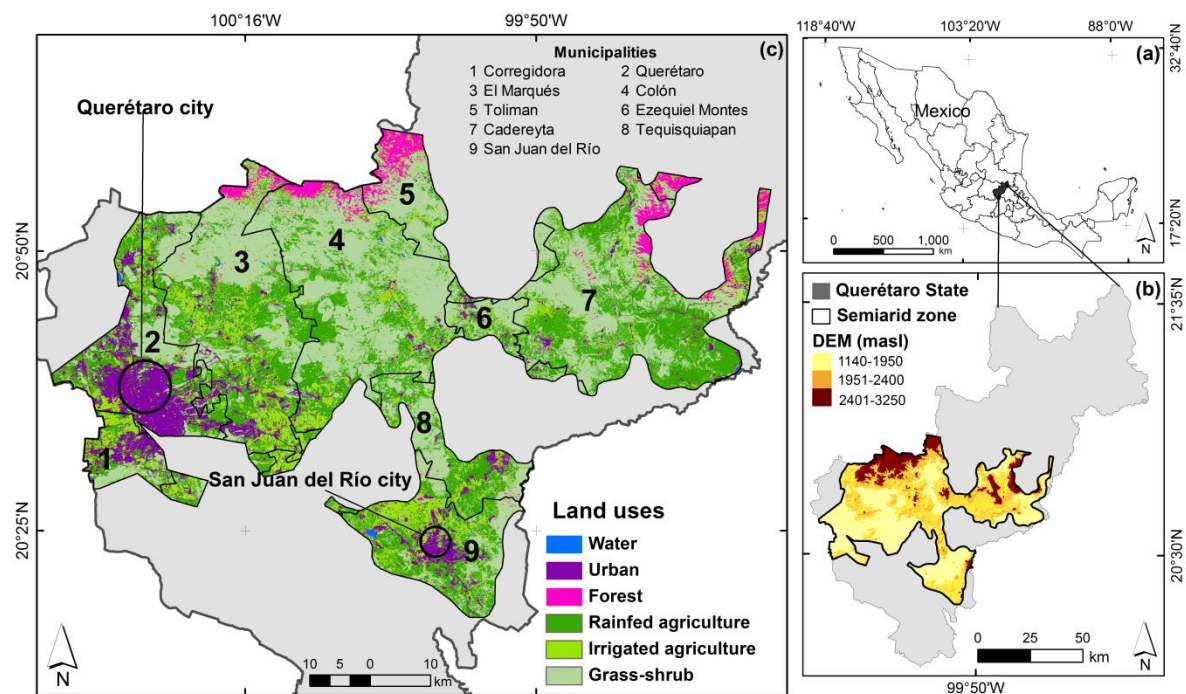


Figure 1. Semi-arid zone of the state of Querétaro (a), digital elevation model (b), and municipal limits and land cover classes (c).

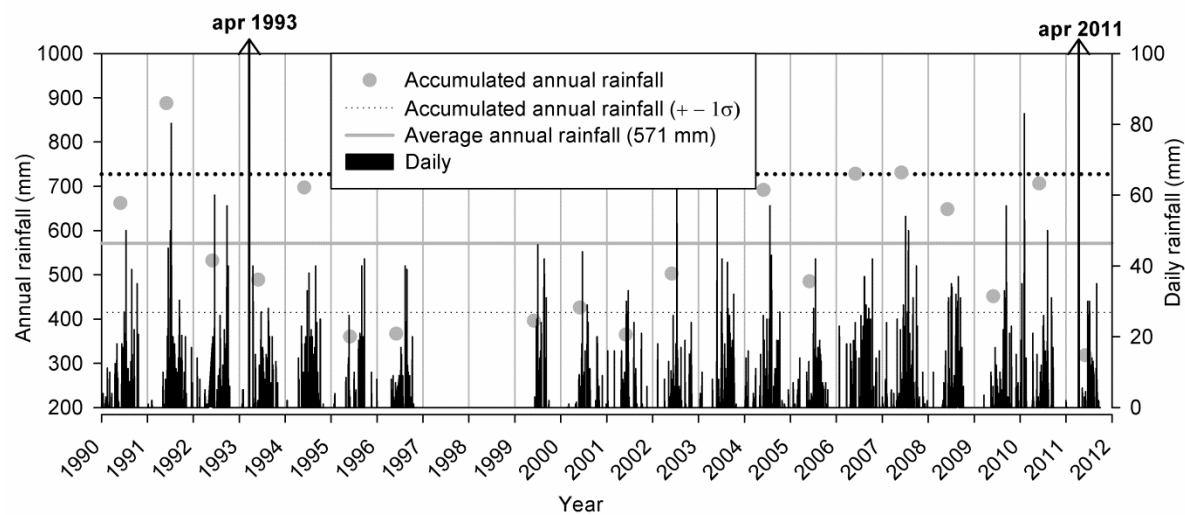


Figure 2. Daily and average annual rainfall from 1980 to 2011 in the semiarid region of the state of Querétaro; arrows indicate the date of the Landsat TM images used for analysis (σ = standard deviation).

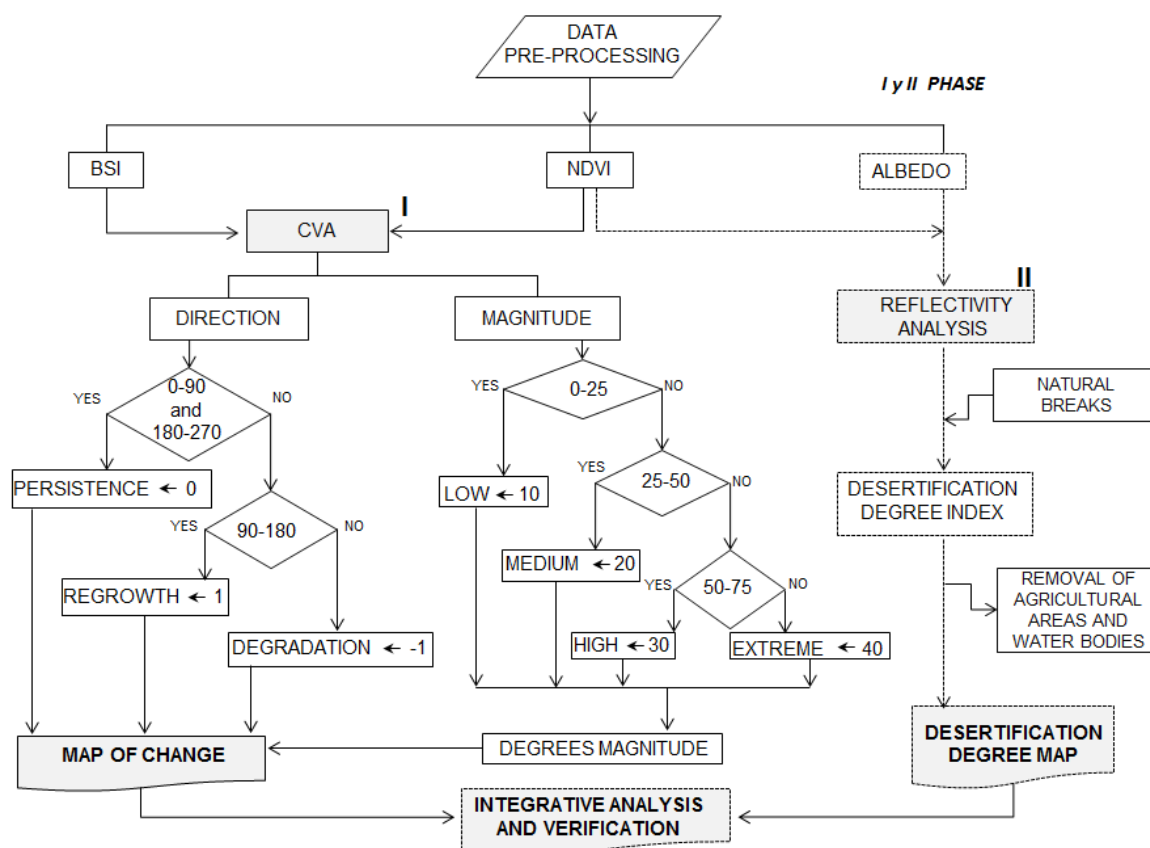


Figure 3. Flow diagram of process for evaluating desertification.

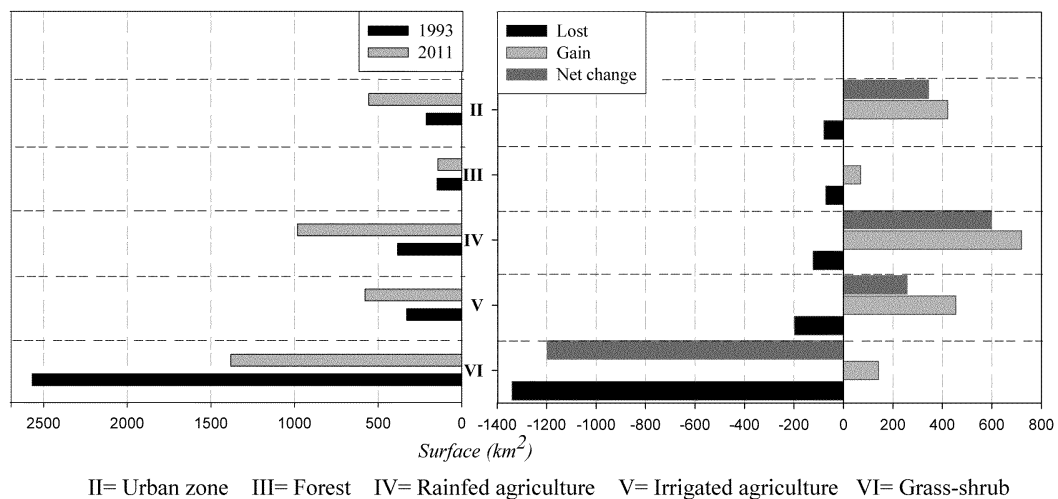


Figure 4. Analysis of change in land cover in the semiarid zone of the state of Querétaro from 1993 to 2011.

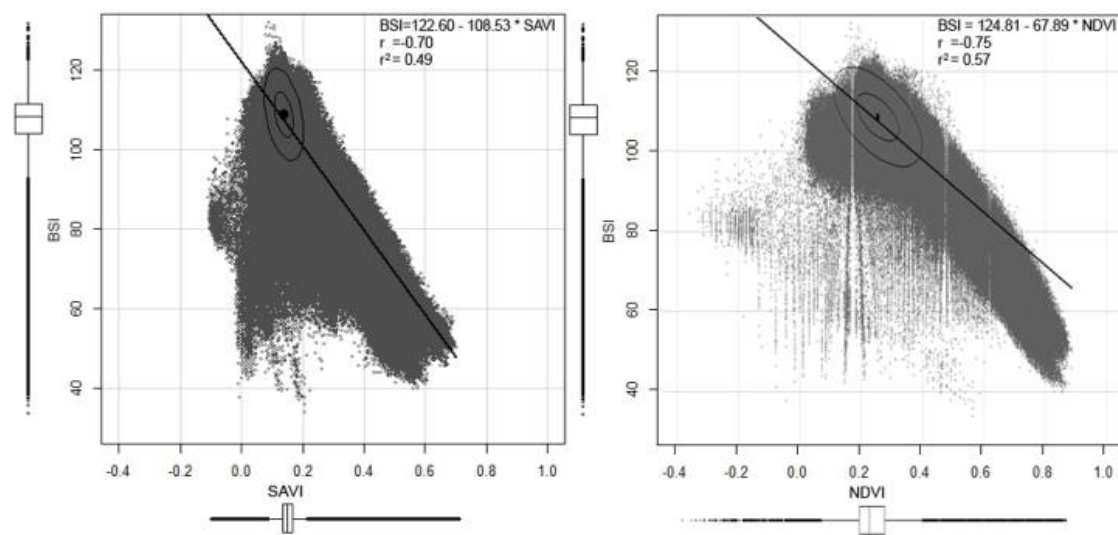


Figure 5. Analysis of the correlation between vegetation indices (SAVI–NDVI) and the bare soil index (BSI).

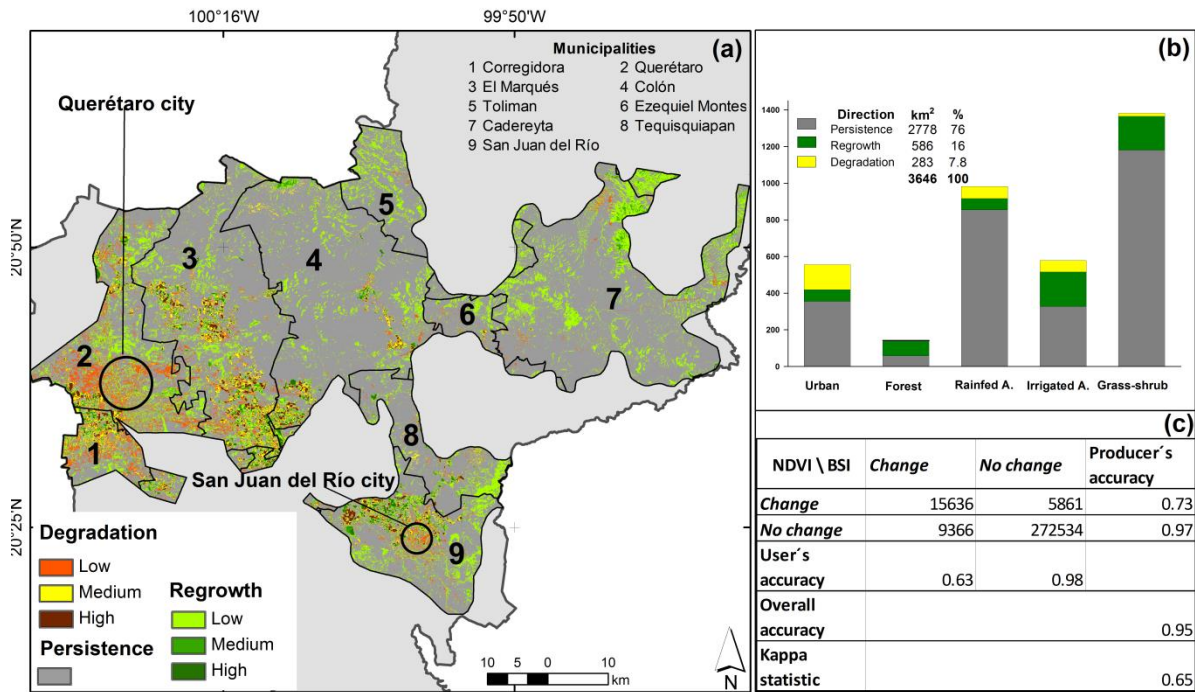


Figure 6. Map of direction and magnitude of changes over the 1993-2011 period (a). Graph of changes in land cover in the semiarid region of the state of Querétaro (b) and confusion matrix of the change detection (c).

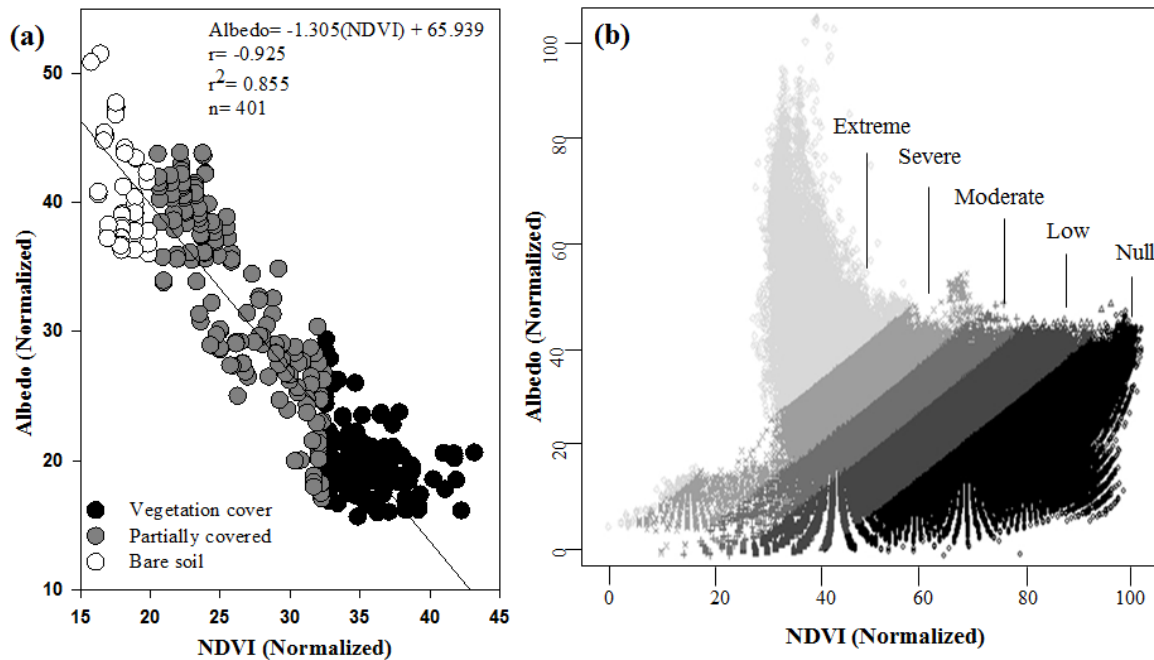


Figure 7. The analysis of the NDVI- α reflectivity correlation; plot of the values for three conditions: bare soil, partially covered, and vegetation cover (a) and the relationship of NDVI- α values and their classification into categories of desertification for the study zone (b).

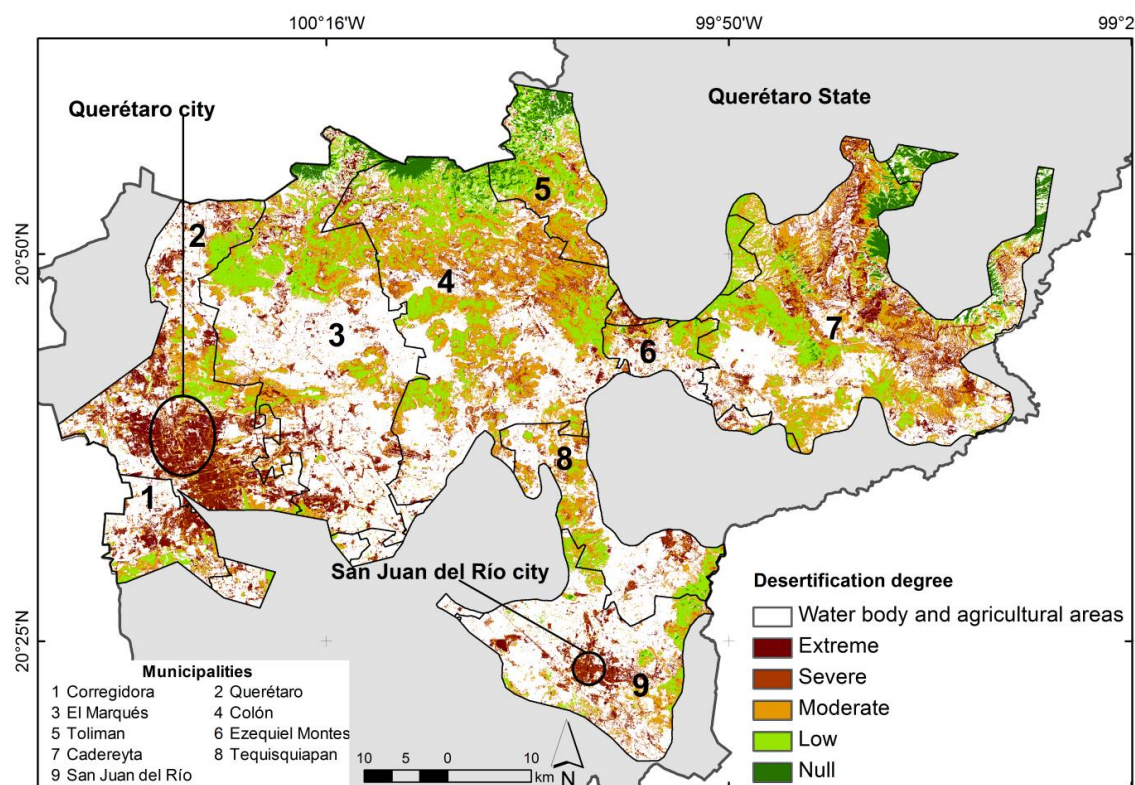


Figure 8. Degree of desertification map corresponding to the evaluated municipalities in the state of Querétaro for 2011.